


Electrical tuning of the band alignment and magnetoconductance in an n-type ferromagnetic semiconductor (In,Fe)As-based spin-Esaki diode

Cite as: Appl. Phys. Lett. **112**, 102402 (2018); <https://doi.org/10.1063/1.5010020>

Submitted: 22 October 2017 . Accepted: 14 January 2018 . Published Online: 07 March 2018

Le Duc Anh, Pham Nam Hai, and Masaaki Tanaka

COLLECTIONS

 This paper was selected as Featured



View Online



Export Citation



CrossMark

ARTICLES YOU MAY BE INTERESTED IN

[A change in sign brings a sign of change for spin-current devices](#)

Scilight **2018**, 100004 (2018); <https://doi.org/10.1063/1.5027513>

[Electrical control of ferromagnetism in the n-type ferromagnetic semiconductor \(In,Fe\)Sb with high Curie temperature](#)

Applied Physics Letters **112**, 122409 (2018); <https://doi.org/10.1063/1.5022828>

[Room temperature microwave oscillations in GaN/AlN resonant tunneling diodes with peak current densities up to 220 kA/cm²](#)

Applied Physics Letters **112**, 103101 (2018); <https://doi.org/10.1063/1.5016414>



Sensors, Controllers, Monitors
from the world leader in cryogenic thermometry



Electrical tuning of the band alignment and magnetoconductance in an n-type ferromagnetic semiconductor (In,Fe)As-based spin-Esaki diode

Le Duc Anh,^{1,2,a)} Pham Nam Hai,^{3,4} and Masaaki Tanaka^{1,4,a)}

¹Department of Electrical Engineering and Information Systems, The University of Tokyo, 7-3-1 Hongo, Bunkyo-ku, Tokyo 113-8656, Japan

²Institute of Engineering Innovation, Graduate School of Engineering, The University of Tokyo, 7-3-1 Hongo, Bunkyo-ku, Tokyo 113-8656, Japan

³Department of Electrical and Electronic Engineering, Tokyo Institute of Technology, 2-12-1 Ookayama, Meguro, Tokyo 152-0033, Japan

⁴Center for Spintronics Research Network (CSRN), The University of Tokyo, 7-3-1 Hongo, Bunkyo-ku, Tokyo 113-8656, Japan

(Received 22 October 2017; accepted 14 January 2018; published online 7 March 2018)

We report a strong bias dependence of the magnetoconductance (MC) of a spin-Esaki diode composed of n⁺-type ferromagnetic semiconductor (FMS) (In,Fe)As and p⁺-type Be doped InAs grown on a p⁺-InAs (001) substrate by molecular beam epitaxy. When the bias voltage V is increased above 450 mV in the forward bias, we found that the MC, measured at 3.5 K under a magnetic field \mathbf{H} of 1 T in the in-plane [110] direction, changes its sign from positive to negative and its magnitude rises rapidly from 0.5% at $V < 450$ mV to -7.4% at $V = 650$ mV. Furthermore, the MC magnitude decreases as $\cos^2(\theta)$ when rotating \mathbf{H} from the in-plane [110] direction to the perpendicular [001] direction, where θ is the angle between \mathbf{H} and the [110] axis. Using a two-fluid model, we explain both the magnitude and the anisotropy of the MC based on the evolution of the spin-Esaki diode's band profile with V . This analysis provides insights into the density of states and spin-polarization of the conduction band and the Fe-related impurity band in n-type FMS (In,Fe)As. Published by AIP Publishing. <https://doi.org/10.1063/1.5010020>

Ferromagnetic semiconductors (FMSs), an important class of materials that inherits the properties of both semiconductors and ferromagnets, provide a straightforward way to integrate spin-related phenomena into semiconductor devices such as diodes and transistors. For their applications, it is very important to characterize the spin-resolved band structure of FMSs. However, among the FMSs studied so far, the spin-splitting in the conduction band (CB) and/or the valence band (VB) of host semiconductors has been convincingly detected in very few materials.^{1,2} Recently, using tunneling spectroscopy in a spin-Esaki diode structure, we have reported a large spontaneous spin splitting (maximum splitting energy $\Delta E \sim 50$ meV at 3.5 K) up to relatively high temperatures (~ 60 K) in the CB of n-type FMS (In,Fe)As.² This was striking because (In,Fe)As is an n-type and narrow-gap FMS,³ where strong ferromagnetism was generally believed to be unfavorable;⁴ yet, there is still plenty of room for increasing the Curie temperature (T_C) of (In,Fe)As.⁵⁻⁷ The tunneling spectroscopy results also indicated that the Fermi level of (In,Fe)As is in the CB, and there is a Fe-related IB located right below the CB bottom.² These previous results, however, have not revealed the spin-polarization of these bands. Detailed knowledge of the spin-dependent band structure is indispensable for understanding the mechanism of ferromagnetism and utilizing n-type FMS (In,Fe)As for spin devices.

In this paper, we investigate the magnetoconductance (MC) of the n⁺-(In,Fe)As/p⁺-InAs-based spin-Esaki diode.² In the diffusive transport regime of magnetic/nonmagnetic p-n

heterojunctions, several intriguing magneto-transport properties, such as spin-voltaic effect, spin-valve effect, and giant MC, were theoretically predicted.⁸⁻¹⁰ Experimentally, giant negative MC has been reported for (In,Mn)As and (In,Mn)Sb-based diodes, whose origins were attributed to the very large effective g -factor of these Mn-doped FMSs.^{11,12} Here, in the n⁺-(In,Fe)As-based spin-Esaki diode, we observe both positive ($\sim 0.5\%$) and negative ($\sim -7.4\%$) MC, whose sign and magnitude depend on the bias voltage V . We attribute the origin of the large negative MC ($\sim -7.4\%$) to the spin dependent band structure of n⁺-(In,Fe)As and the Zeeman splitting in p⁺-InAs, which is sizable owing to the large g -factor ($g_{\text{InAs}} = -15$).¹³ We show that under a magnetic field, p⁺-InAs works as a spin-sensitive probe and that the bias-dependence of the MC sign and magnitude can reveal the energy and spin-dependence of the density of states (DOS) of n⁺-(In,Fe)As.

The spin-Esaki diode structure examined in this study is, from the top surface, 50 nm-thick n⁺-type (In,Fe)As (6% Fe)/5 nm-thick InAs/250 nm-thick p⁺-type InAs:Be (the Be concentration is $1 \times 10^{18} \text{ cm}^{-3}$)/p⁺-type InAs (001) substrate grown by molecular beam epitaxy [Fig. 1(a)]. T_C of the (In,Fe)As layer is 45 K. The sample was then patterned into mesa diodes with a diameter of 200 μm for I - V measurements. The bias polarity was defined so that under the positive bias, the current flows from the p⁺-type InAs substrate to the top n⁺-type (In,Fe)As layer. The details of the growth, process, and characterization of the device were described elsewhere.²

Band profiles of the spin-Esaki diode at different V values are illustrated in Fig. 1(b), where E_n and E_p are the quasi-Fermi levels of n⁺-(In,Fe)As and p⁺-InAs, respectively, and

^{a)} Authors to whom correspondence should be addressed: anh@cryst.t.u-tokyo.ac.jp and masaaki@ee.t.u-tokyo.ac.jp

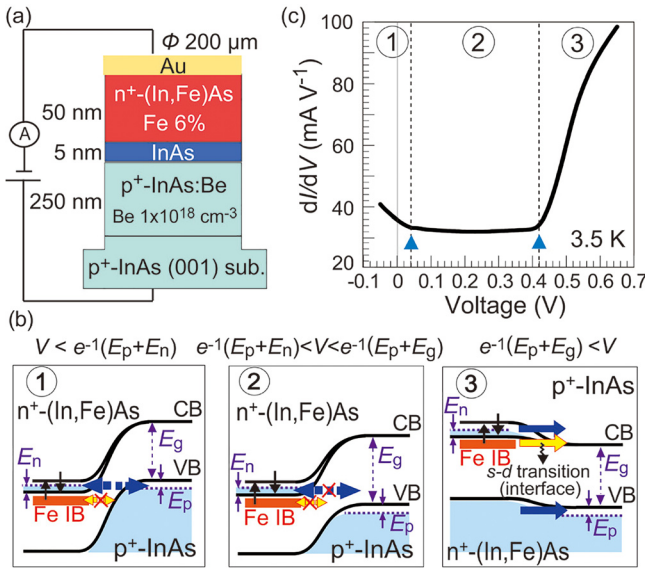


FIG. 1. (a) Schematic device structure and measurement configuration of the spin-Esaki diode. (b) The band profile of the pn junction in the three regions: ①: Tunneling region, ②: Bandgap region, and ③: Diffusion region. The $n^+(\text{In,Fe})\text{As}$ conduction band (CB) is spin-split, and only one spin band is occupied. E_g is the bandgap energy of InAs and (In,Fe)As, and E_n and E_p are the quasi-Fermi levels in the $n^+(\text{In,Fe})\text{As}$ and $p^+\text{-InAs}$ electrodes, respectively. The Fe-related impurity band (IB) (orange) lies right below the CB bottom. (c) dI/dV - V characteristics measured at 3.5 K. The borders between three regions are indicated by the blue triangles at 40 mV and 420 mV.

$E_g = 0.42$ eV is the bandgap of both $n^+(\text{In,Fe})\text{As}$ and $p^+\text{-InAs}$ (We assume that the bandgaps of $n^+(\text{In,Fe})\text{As}$ and $p^+\text{-InAs}$ are equal). From the tunneling spectroscopy results,² we know $E_n = 20$ meV and $E_p = 8$ meV. Note that in the CB of $n^+(\text{In,Fe})\text{As}$ of this spin-Esaki diode, the spin-splitting energy at 3.5 K is 32 meV, and thus, only one type of spin electron fills up the CB bottom (the half-metallic band structure). Our results also indicated the existence of a Fe-related impurity band (IB) below the CB bottom of (In,Fe)As. At $V < e^-(E_n + E_p)$ (e is the elementary charge), corresponding to region ① (tunneling region), electrons tunnel from the CB of $n^+(\text{In,Fe})\text{As}$ to the VB of $p^+\text{-InAs}$. Note that the tunneling from the Fe-related IB of (In,Fe)As to the VB top of $p^+\text{-InAs}$ is prohibited by the different orbital symmetry of the two bands. At $e^-(E_n + E_p) < V < e^-(E_g + E_p)$, corresponding to region ② (bandgap region), the (In,Fe)As CB bottom is lifted above the VB top of $p^+\text{-InAs}$, and thus, the current due to the CB-to-VB tunnelling is suppressed. Finally, at $e^-(E_g + E_p) < V$, corresponding to region ③ (diffusion region), the occupied states in the CB (or VB) and IB of $n^+(\text{In,Fe})\text{As}$ reach the same energies as the unoccupied states in the CB (or VB) of $p^+\text{-InAs}$, and then, diffusive and drift currents start to flow. Therefore, by changing V , we can switch the transport mechanism (tunneling \leftrightarrow diffusive) and the participating bands (CB, VB, or IB) of the current. This is an important advantage of this FMS-based spin-Esaki diode. The dI/dV - V curve measured at 3.5 K of the diode is shown in Fig. 1(c), in which all three regions are clearly observed (the two transition borders are indicated by blue triangles).

We measure the magnetic field (\mathbf{H}) dependence of the spin-Esaki diode's conductance σ at various V values. First, we fix the magnetic field direction in the [110] direction (in the film plane) and measure the magnetic field strength (H)-dependence

of σ at 3.5 K [Figs. 2(a) and 2(b)]. Here, we define the MC ratio at H as $\text{MC}(H) = [\sigma(H) - \sigma(H = 0T)]/\sigma(H = 0T) \times 100(\%)$. In regions ① and ②, a small positive MC ($\sim 0.5\%$ at 1 T) is observed and remains nearly unchanged with V . In region ③, the MC ratio retains its positive sign at small V values ($420 \text{ mV} \leq V \leq 450 \text{ mV}$). However, at $V = 460 \text{ mV}$, a small negative MC component starts to appear and overlaps with the existing positive one, as can be seen in Fig. 2(b). The negative MC's magnitude grows rapidly as V is increased above 460 mV and reaches a saturated value of -7.4% at 1 T when $V = 650 \text{ mV}$. The evolution of the MC magnitude with V is summarized in Fig. 2(c), where one can see the sign reversal occurring at around $V = 450 \text{ mV}$. Next, we measure the MC in several \mathbf{H} directions between the [110] direction (in the film plane) and the [001] direction (perpendicular to the film plane). We define θ as the angle between \mathbf{H} and the [110] axis. At $V < 450 \text{ mV}$, the small positive MC does not change with θ [Fig. 3(a)]. There is also a small negative MC that is quadratic to the magnetic field strength projected in the [100] axis, which originates from the Lorentz force in the $p^+\text{-InAs}$ substrate (see supplementary material). However, at $V > 450 \text{ mV}$, the negative MC decreases with increasing θ , as shown in Fig. 3(b) for $V = 500 \text{ mV}$. At a fixed H , the conductance σ depends on θ as: $\sigma(\theta) = \sigma(90^\circ) - [\sigma(90^\circ) - \sigma(0^\circ)] \cos^2(\theta)$ [see Fig. 3(c) for $H = 1 \text{ T}$, and note that the contribution from the quadratic negative MC is excluded from the raw MC magnitude]. The $\cos^2(\theta)$ -angle dependence is similar to that of the anisotropic magnetoresistance (AMR) in ferromagnetic metals¹⁴ and FMS (Ga,Mn)As.¹⁵ This result will be discussed and explained later.

The turning point (sign change) of the H -dependence of σ , which is 450 mV [Figs. 2(b) and 2(c)], is not coincident with the starting point of the diffusion region ($\sim 420 \text{ mV}$).

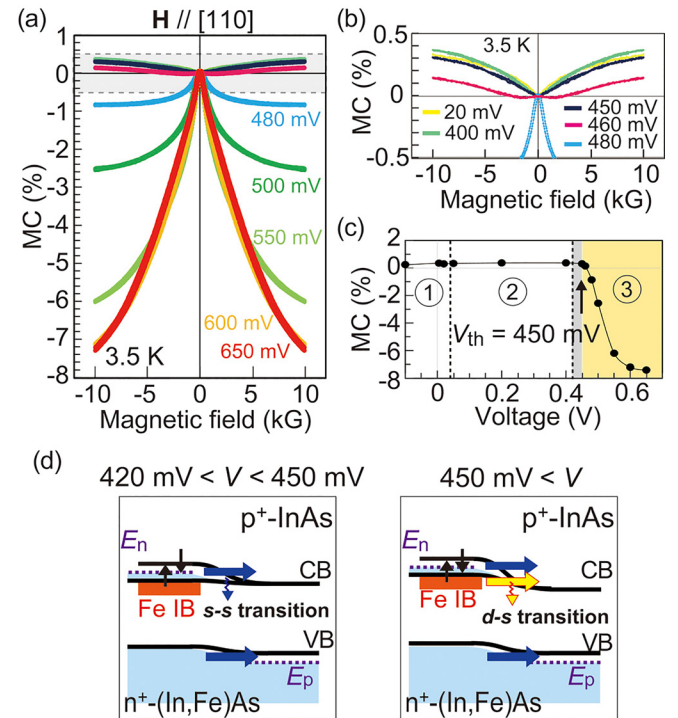


FIG. 2. (a) Magnetoconductance (MC) of the spin-Esaki diode at various bias voltages V , measured at 3.5 K with a magnetic field \mathbf{H} applied in the [110] direction in the film plane. (b) Magnified plot of the positive MCs in (a). (c) V -dependence of MC at 3.5 K. (d) The band profile of the pn junction at $420 \text{ mV} < V < 450 \text{ mV}$ (left) and $450 \text{ mV} < V$ (right).

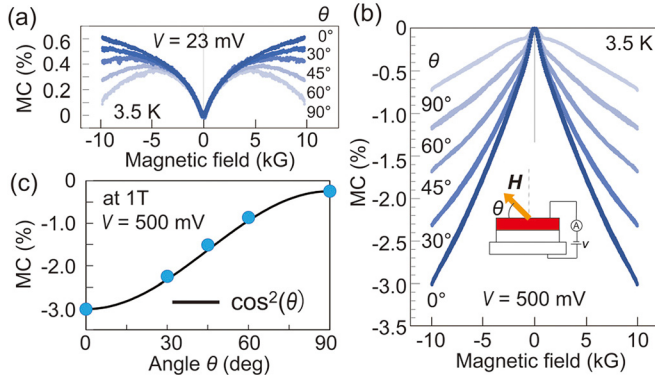


FIG. 3. Evolution of the MC of the spin-Esaki diode when the magnetic field \mathbf{H} is applied in various directions between the [110] and [001] axes. Here, θ is the angle between \mathbf{H} and the [110] axis. MC vs. magnetic field with various θ values (a) at $V = 23$ mV and (b) at $V = 500$ mV. The inset of (b) shows the measurement geometry. (c) θ -dependence of the MC magnitude at 1 T (blue points), which can be approximated by $\cos^2(\theta)$ (black curve). All were measured at 3.5 K.

This indicates that the origin of this bias-dependence is not simply the different transport mechanisms (tunneling vs. diffusive). As shown in Fig. 2(d), considering that the quasi-Fermi energy E_n of (In,Fe)As is 20 meV, one can deduce that at $V = 420$ – 450 mV, the empty CB of p^+ -InAs is aligned with the CB bottom of n^+ -(In,Fe)As but still has higher energy than the Fe-related IB. Thus, in this bias range, electrons only flow between the s -symmetry orbitals at the pn junction interface.¹⁶ However, at $V > 450$ mV, electrons from the d -symmetry IB start to flow towards the CB of p^+ -InAs.² We believe that this participation of the IB's electrons in the current at $V > 450$ mV plays the central role in this peculiar evolution of the MC in our spin-Esaki diode.

We use a two-fluid model to quantitatively describe the observed MC. Because n^+ -(In,Fe)As and p^+ -InAs are highly doped and metallic, the bias voltage V mainly drops at the pn junction interface. Therefore, for simplicity, we only consider the change in σ occurring at the n^+ -(In,Fe)As/ p^+ -InAs interface. Since the pn interface thickness is much smaller than the spin diffusion length of InAs,¹⁷ the overall σ of the diode can be decomposed into the conductance of the up-spin angular momentum (σ_{\uparrow} , aligned with \mathbf{H}) and down-spin angular momentum (σ_{\downarrow} , anti-aligned with \mathbf{H}) channels: $\sigma = \sigma_{\uparrow} + \sigma_{\downarrow}$. Here, the quantization axis is along \mathbf{H} . At $V > 420$ mV, σ_{γ} (here, $\gamma = \uparrow$ or \downarrow is the spin angular momentum) is proportional to the filled density of states $N_{(\text{In,Fe})\text{As}}$ in n^+ -(In,Fe)As, the empty density of states N_{InAs} in p^+ -InAs, and the transition probability T_{d-s} (T_{s-s}) between the IB (CB) of n^+ -(In,Fe)As and the CB of p^+ -InAs of the same spin at the interface, if we assume spin-conserved transitions at the pn interface,

$$\sigma_{\gamma} \propto (N_{s,\gamma,(\text{In,Fe})\text{As}} T_{s,\gamma-s,\gamma} + N_{d,\gamma,(\text{In,Fe})\text{As}} T_{d,\gamma-s,\gamma}) \times N_{s,\gamma,\text{InAs}}. \quad (1)$$

Here, s and d indicate the orbital symmetry of the carriers. The first and second terms in the brackets of Eq. (1) are the contributions of the flows of the s -orbital and d -orbital electrons of the n^+ -(In,Fe)As side towards the s -orbital states in the p^+ -InAs side, respectively. With increasing V above 450 mV, the contribution of the second term is increased due to the increase in $N_{d,\gamma,(\text{In,Fe})\text{As}}$, as shown in Fig. 2(d).

At 3.5 K, under a strong magnetic field \mathbf{H} , the band structure of the ferromagnetic (In,Fe)As layer is unchanged,² while that of p^+ -InAs exhibits a small Zeeman splitting of $\Delta E = g\mu_B H$, where μ_B is the Bohr magneton and g is the g -factor of InAs. According to the Boltzmann distribution, this ΔE induces changes in $N_{s,\text{InAs}}$ as $\exp\left(-\frac{g\mu_B H}{k_B T}\right)$ and $\exp\left(\frac{g\mu_B H}{k_B T}\right)$ for up-spin and down-spin electrons, respectively. Consequently, the overall conductance σ at a fixed bias V changes with H ,

$$\sigma(H) = \frac{\sigma_{\uparrow} \exp\left(-\frac{g\mu_B H}{k_B T}\right) + \sigma_{\downarrow} \exp\left(\frac{g\mu_B H}{k_B T}\right)}{\cosh\left(\frac{g\mu_B H}{k_B T}\right)}. \quad (2)$$

Here, k_B is the Boltzmann constant. Hence, the MC of the spin-Esaki diode at 3.5 K under a magnetic field strength H is given by

$$\begin{aligned} \text{MC} (\%) &= \frac{\sigma(H) - \sigma(0)}{\sigma(0)} \times 100 \\ &= \frac{\sigma_{\downarrow} - \sigma_{\uparrow}}{\sigma_{\downarrow} + \sigma_{\uparrow}} \tanh\left(\frac{g\mu_B H}{k_B T}\right) \times 100. \end{aligned} \quad (3)$$

Thus, the sign and magnitude of the MC are determined by the difference in the two spin-channels' conductance $\sigma_{\downarrow} - \sigma_{\uparrow}$, which is related to the spin polarization of the corresponding (In,Fe)As bands. We define $\frac{\sigma_{\downarrow} - \sigma_{\uparrow}}{\sigma_{\downarrow} + \sigma_{\uparrow}} = \beta \frac{M(H)}{M_S}$, where β is the spin asymmetry coefficient, similar to that introduced by Valet and Fert,¹⁸ and $M(H)/M_S$ is the magnetization of (In,Fe)As normalized by its saturated value, which was added to take into account the multi-domain structure in the (In,Fe)As layer (see [supplementary material](#)). Using $g = -15$ of InAs and β as the only fitting parameter, we are able to calculate and well reproduce the MC behavior [Fig. 4(a)]. The obtained β value, shown in Fig. 4(b), changes its sign from negative to positive at $V = 450$ mV, significantly increases at $V > 450$ mV, and reaches a saturated value of 0.075 at $V = 650$ mV. This indicates a strong enhancement of σ_{\downarrow} at $V = 450$ – 650 mV, caused by the participation of the Fe-related IB below the CB bottom of (In,Fe)As. This implies that the Fe-related IB must contain mainly electrons with down-spin angular momentum, and the band width is around 200 meV. In the same fashion, the small negative β at $V = 420$ – 450 mV suggests the opposite spin polarization in the CB edge of (In,Fe)As. In this region ($V < 450$ mV), however, the MC intensity is small and comparable to the positive MC typically observed in the (In,Fe)As bulk. Therefore, further investigations are still required to confirm the sign of the spin polarization in the CB edge of (In,Fe)As.

The two-fluid model and the deduced spin-dependent band structure of (In,Fe)As can also qualitatively explain the anisotropic behavior of the MC in Fig. 3, if one takes into account the effect of spin-orbit interaction (SOI). As illustrated in Fig. 4(c), at the pn junction interface at $V > 450$ mV, besides the spin-conserved electron flow from the down-spin d orbitals to the down-spin s orbitals ($d_{\downarrow} \rightarrow s_{\downarrow}$) that constitutes σ_{\downarrow} , a flow accompanying the spin-flip process

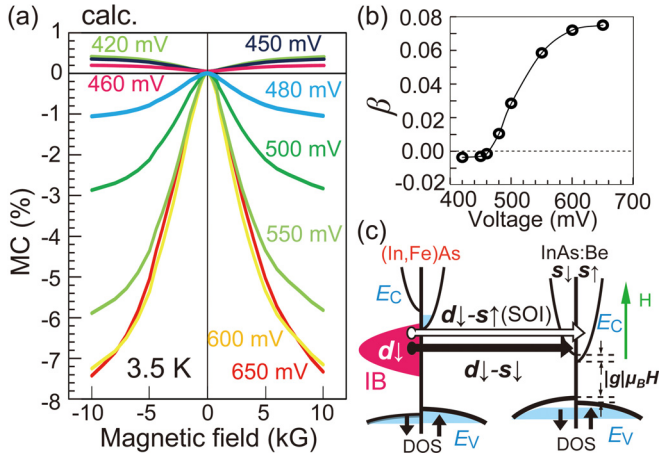


FIG. 4. (a) MC curves of the spin-Esaki diode at various V values calculated by the two-fluid model. (b) Spin asymmetry coefficient β obtained from the fitting in (a). (c) The spin-dependent band structures of $n^+(\text{In,Fe})\text{As}$ and $p^+\text{-InAs}$ deduced from the MC results. Under a magnetic field H , the band structure of $p^+\text{-InAs}$ splits by $\Delta E = |g|\mu_B H$, while that of $n^+(\text{In,Fe})\text{As}$ is unchanged. At $V > 450$ mV, there are two main electron flows at the pn interface: The spin-conserved flow from the down-spin d orbitals to the down-spin s orbitals ($d\downarrow-s\downarrow$, black arrow) and the flow accompanying the spin-flip process due to SOI from the down-spin d orbitals to the up-spin s orbitals ($d\downarrow-s\uparrow$, open arrow).

due to SOI from the down-spin d orbitals to the up-spin s orbitals ($d\downarrow-s\uparrow$) also co-exists and enhances σ_\uparrow . Similar to the s - d scattering theory in metallic ferromagnets,¹⁹ in all five d -orbitals ($|m_S = 0, \pm 1, \pm 2\rangle$) of the Fe atoms, the SOI-induced spin-flip $d\downarrow-s\uparrow$ transition probability is highest when an s -orbital electron is transferred from the $|m_S = 0\rangle$ orbital because the effect of SOI on this orbital is strongest. Moreover, the probability of the $|s\rangle \rightarrow |m_S = 0\rangle$ transition is largest when the magnetization is parallel to the current direction,¹⁹ which corresponds to $\theta = 90^\circ$ in our case. Therefore, when one rotates θ from 0° to 90° , σ_\uparrow increases and σ_\downarrow decreases owing to the stronger ($d\downarrow-s\uparrow$) process. Consequently, β decreases and becomes close to 0, which decreases the absolute magnitude of MC close to 0 (MC = -3.0% at $\theta = 0^\circ$ to MC = -0.7% at $\theta = 90^\circ$). This anisotropic d - s transition mechanism manifests itself in the $\cos^2(\theta)$ -dependence of the MC in Fig. 3(c), similar to that of AMR in metallic ferromagnets.^{14,15,19}

In summary, we have reported strong spin-dependent transport behavior in the MC of an $(\text{In,Fe})\text{As}$ -based spin-Esaki diode, in which the MC exhibits a sign reversal at $V = 450$ mV and the negative MC ratio rapidly increases at $V > 450$ mV. The contribution of electrons in the IB below the CB bottom of

$n^+(\text{In,Fe})\text{As}$ to the current is the origin of this observed behavior. This work vividly demonstrates that in FMS-based diode structures, magnetotransport phenomena can be tuned by selecting the band components participating in the current using device structure design and/or bias voltage. This feature leads to physics and device functionalities that are promising for spintronic device applications.

See [supplementary material](#) for more detailed information on sample characterization and data on the temperature dependence of magnetoconductance.

This work was partly supported by Grants-in-Aid for Scientific Research (Nos. 26249039 and 17H04922), CREST of JST, and the Spintronics Research Network of Japan (Spin-RNJ). L.D.A. acknowledges support from the Murata Science Foundation. P.N.H. acknowledges support from the Kato Foundation for Promotion of Science.

- ¹H. Boukari, P. Kossacki, M. Bertolini, D. Ferrand, J. Cibert, S. Tatarenko, A. Wasiela, J. A. Gaj, and T. Dietl, *Phys. Rev. Lett.* **88**, 207204 (2002).
- ²L. D. Anh, P. N. Hai, and M. Tanaka, *Nat. Commun.* **7**, 13810 (2016).
- ³P. N. Hai, L. D. Anh, S. Mohan, T. Tamegai, M. Kodzuka, T. Ohkubo, K. Hono, and M. Tanaka, *Appl. Phys. Lett.* **101**, 182403 (2012).
- ⁴T. Dietl, F. Matsukura, and H. Ohno, *Phys. Rev. B* **63**, 195205 (2001).
- ⁵P. N. Hai, L. D. Anh, and M. Tanaka, *Appl. Phys. Lett.* **101**, 252410 (2012).
- ⁶L. D. Anh, P. N. Hai, and M. Tanaka, *Appl. Phys. Lett.* **104**, 042404 (2014).
- ⁷L. D. Anh, P. N. Hai, Y. Kasahara, Y. Iwasa, and M. Tanaka, *Phys. Rev. B* **92**, 161201(R) (2015).
- ⁸I. Žutić, J. Fabian, and S. Das Sarma, *Phys. Rev. Lett.* **88**, 066603 (2002).
- ⁹N. Bebedeva and P. Kuivalainen, *J. Appl. Phys.* **93**, 9845 (2003).
- ¹⁰I. Žutić, J. Fabian, and S. Das Sarma, *Rev. Mod. Phys.* **76**, 323 (2004).
- ¹¹S. J. May and B. W. Wessels, *J. Vac. Sci. Technol. B* **23**, 1769 (2005).
- ¹²J. A. Peters, N. Rangaraju, C. Feeser, and B. W. Wessels, *Appl. Phys. Lett.* **98**, 193506 (2011).
- ¹³C. R. Pigeon, D. L. Mitchell, and R. N. Brown, *Phys. Rev.* **154**, 737 (1967).
- ¹⁴T. R. McGuire, J. A. Aboaf, and E. Klokholm, *IEEE Trans. Magn.* **20**, 972 (1984).
- ¹⁵A. W. Rushforth, K. Výborný, C. S. King, K. W. Edmonds, R. P. Campion, C. T. Foxon, J. Wunderlich, A. C. Irvine, P. Vašek, V. Novák, K. Olejník, J. Sinova, T. Jungwirth, and B. L. Gallagher, *Phys. Rev. Lett.* **99**, 147207 (2007).
- ¹⁶P. N. Hai, D. Sasaki, L. D. Anh, and M. Tanaka, *Appl. Phys. Lett.* **100**, 262409 (2012).
- ¹⁷T. F. Boggess, J. T. Olesberg, C. Yu, M. E. Flatte, and W. H. Lau, *Appl. Phys. Lett.* **77**, 1333 (2000).
- ¹⁸T. Valet and A. Fert, *Phys. Rev. B* **48**, 7099 (1993).
- ¹⁹S. Kokado, M. Tsunoda, K. Harigaya, and A. Sakuma, *J. Phys. Soc. Jpn.* **81**, 024705 (2012).